

## Crystal Structure of the High-Pressure Phase Silicon VI

M. Hanfland

*European Synchrotron Radiation Facility, BP 220, F-38043 Grenoble, France*

U. Schwarz and K. Syassen

*Max-Planck-Institut für Festkörperforschung, Heisenbergstrasse 1, 70569 Stuttgart, Germany*

K. Takemura

*National Institute for Research in Inorganic Materials, Tsukuba, Ibaraki 305-0044, Japan*

(Received 1 October 1998)

The crystal structure of Si was studied at pressures between 30 and 50 GPa using high-resolution monochromatic synchrotron x-ray diffraction. The powder diffraction patterns of the phase Si VI are indexed on the basis of an orthorhombic unit cell containing 16 atoms. The space group is assigned as *Cmca*. Full profile refinements reveal that Si VI is isotopic to Cs V; i.e., axial ratios and atomic coordinates are nearly identical for both phases. Thus, formation of the Cs V type structure is not a unique feature of the pressure-driven electronic *s-d* transition in Cs. Instead, the structure type appears to be more common, occurring intermediate between 8- and 12-fold coordinated structures. [S0031-9007(98)08345-8]

PACS numbers: 62.50.+p, 61.50.Ks, 61.66.Bi, 64.70.Kb

Silicon plays a prominent role in the study of pressure-induced phase transitions of elemental solids. A large variety of crystal structures and chemical bonding situations is encountered along the route from the tetrahedrally coordinated diamond-type structure towards close packing of atoms at very high pressures [1–8]. At least ten phases with different crystal structures are known to exist [9]. The simple electronic configuration of Si, involving mainly *sp* orbitals, makes it a highly attractive material for first-principles calculations of phase stability and related lattice dynamical properties [10–17]. With increasing pressure Si transforms to the tetragonal  $\beta$ -Sn structure near 12 GPa [2], which until recently was thought to transform directly to the primitive hexagonal (ph) structure at 16 GPa [3–6]. In agreement with theoretical considerations [11,12] an angle-dispersive synchrotron x-ray diffraction study revealed the existence of an intermediate orthorhombic phase between 13 and 16 GPa (space group *Imma*,  $Z = 4$  atoms per cell) [8]. Above 42 GPa a hexagonal close-packed (hcp) structure has been observed [3,5–7] which transforms to a face centered cubic (fcc) at 78 GPa [6,7]. All these high-pressure phases are metals [1,18] and superconductivity has been predicted and observed in several of them [11–13,19–21].

A long-standing question is the structure of the phase Si VI, which exists near 40 GPa [3,7], intermediate between the 8-fold coordinated ph and the 12-fold coordinated hcp phases. Si VI shows a superconducting transition temperature significantly higher than the neighboring ph and hcp phases [21]. The structure of Si VI was first assumed to be double hexagonal close packed (dhcp) [22], i.e., a mixed hcp- and fcc-like stacking of close-packed hexagonal layers. Early theoretical studies supported the restacking of hexagonal close-packed layers [12]. Alternatively,

orthorhombic structures with  $Z = 4$  were proposed [23]. A more recent energy-dispersive synchrotron diffraction study showed that both structural assignments are incorrect [7].

In this Letter we report a solution for the Si VI structure and the pressure dependence of its structural parameters. Results are based on angle-dispersive powder diffraction data measured at a third generation synchrotron source. Because of the excellent resolution, the patterns could be indexed reliably on the basis of a large orthorhombic unit cell containing 16 atoms. The space group is found to be *Cmca*. Structural refinements show that Si VI is isotopic to the high pressure phase Cs V, whose structure was solved only recently [24].

The diffraction studies of Si were performed in the pressure range from 30 to 50 GPa using a diamond anvil cell (DAC) in combination with the ruby luminescence method [25] for pressure measurement. Experiments were carried out at the ID9 beam line of the European Synchrotron Radiation Facility, Grenoble, using monochromatic radiation and image plate detection. X rays from an undulator source were focused vertically by a Pt-coated Si mirror and horizontally by an asymmetrically cut bent Si(111) Laue monochromator [26]. At the wavelength used in this study [0.448 64(4) Å, energy 27.639 keV]  $\sim 1 \times 10^{11}$  photons/s are delivered into the  $30 \times 30 \mu\text{m}^2$  focal spot, a gain in flux by about a factor of 100 compared to second generation synchrotrons. Image plates were placed at a large distance (450 mm) from the sample, resulting in an extraordinarily high instrumental resolution, characterized by a normalized width (FWHM) of diffraction peaks of  $\Delta\Theta/\Theta = 2 \times 10^{-3}$  at a diffraction angle of  $2\Theta = 20^\circ$ . Exposure times were 3 min. To improve powder averaging, the DAC was

rocked by  $\pm 3^\circ$ . Conventional diffraction diagrams were obtained by suitable integration of the two-dimensional images [27]. The Si sample (National Institute of Standards and Technology powder diffraction reference material) was loaded into the DAC together with argon as the pressure medium. After each pressure increase the DAC was annealed for 1 hour at 115 °C. The widths of Si diffraction lines were small and close to the instrumental resolution, indicating a negligible residual stress. Ar diffraction linewidths were large and strongly varying for different reflections, probably due to stacking faults.

Diffraction diagrams measured at different pressures are shown in Fig. 1. The diffraction lines are unambiguously assigned to the different phases of Si and to the Ar medium (fcc structure [28]) by following their evolution with pressure. Below 38 GPa only the ph phase of Si was observed. Appearance of additional diffraction lines at 38 GPa indicated the onset of the transition to Si VI in agreement with previous studies [7]. Above 40 GPa the diffraction lines of ph Si had disappeared and the Si VI pattern together with developing peaks of hcp Si were observed. Upon further increasing the pressure hcp lines gained intensity at the expense of Si VI lines. At 49.2 GPa traces of Si VI were still detectable.

A diffraction pattern of Si VI measured at 42.5 GPa is shown in Fig. 2. Ar reflections were subtracted to fa-

cilitate the analysis. At this pressure only weak lines from hcp Si were observed. The pattern can be indexed assuming an orthorhombic cell containing 16 atoms. Corresponding Miller indices are given in Fig. 2(a). Earlier studies [3,7] failed to determine the correct unit cell, partly because the extremely weak (200) reflection [see inset of Fig. 2(b)] as well as the (020) and (002) reflections, which are essential for determining the type and size of the unit cell, were not observed, and no indication was seen for three overlapping reflections contributing to the strongest peak [29]. The high-resolution and improved sensitivity resulting from the use of a third generation synchrotron x-ray source thus is indispensable for a reliable indexing of high-pressure diffraction data of low-symmetry phases with large unit cells.

The only centrosymmetric space group (SG) consistent with the systematic extinctions of Bragg reflections was determined to be  $Cmca$ . A structure with this SG and  $Z = 16$  is not known for any element at ambient conditions. However, such a structure was found recently for the high pressure phase Cs V [24]. In Cs V the atoms occupy the  $8f$  and  $8d$  Wyckoff positions of  $Cmca$ . By visual inspection, the diffraction peak intensities of Si VI very closely resemble those of Cs V. The Cs V structure model was therefore tried as a starting point for refining the structural parameters of Si VI based on 31 reflections. Since Si VI was always found to coexist with either ph (SG  $P6/mmm$ ) or hcp-Si (SG  $P6_3/mmc$ ), two-phase refinements were performed using GSAS [30]. Excellent agreement between calculated and measured patterns is achieved [compare Fig. 2(b)] if preferred orientation is

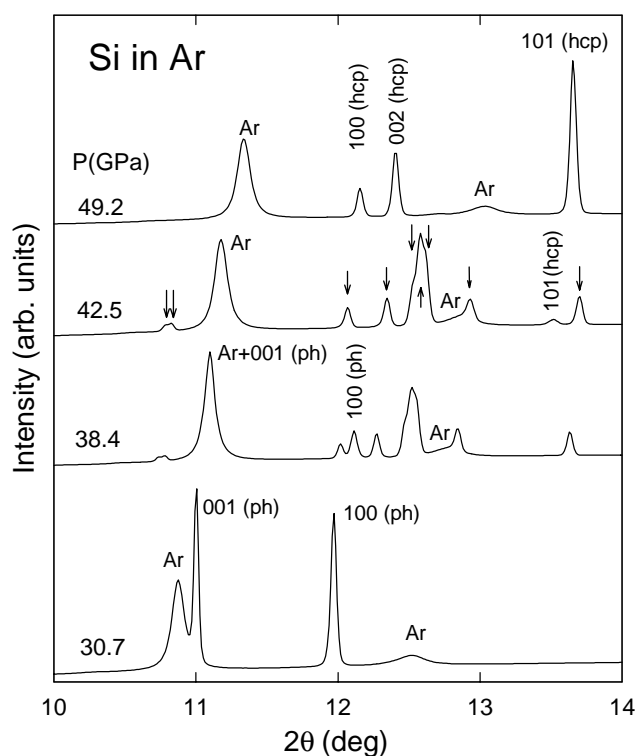


FIG. 1. Angle-dispersive x-ray diffraction patterns of Si at different pressures. Ar was used as the pressure medium. The sequence is ph Si (30.7 GPa), Si VI coexisting with ph Si (38.4 GPa), Si VI with a small admixture from hcp Si (42.5 GPa, arrows indicate Si VI reflections), and hcp Si (49.2 GPa).

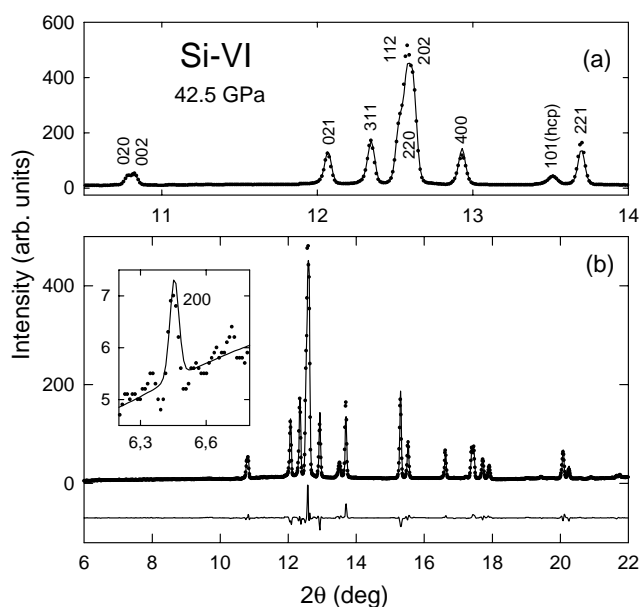


FIG. 2. Diffraction pattern of Si VI at 42.5 GPa. Ar reflections have been subtracted. (a) Expanded view with indexing of Bragg peaks and (b) the full diagram plotted together with the difference between the measured and the refined patterns. The inset shows the weak (200) reflection.

taken into account [31]. The refined structural parameters for Si VI are listed in Table I. Also listed are the corresponding parameters for Cs V at 12 GPa. It is important to note that Si VI and Cs V are not only isostructural, but have almost identical axial ratios and positional parameter values. In particular, the same small deviation from tetragonal symmetry is found for Si VI. In Pearson notation the structure is denoted oC16. For figures showing the full structure and its relation to the fcc structure we refer to Ref. [24].

In the oC16 structure flat layers of  $8f$  atoms alternate along the [100] direction with buckled layers of  $8d$  atoms, see Fig. 3. The unit cell extends over four layers. The  $8f$  atoms are 11-fold coordinated by five  $8f$  and six  $8d$  neighbors, the  $8d$  atoms are 10-fold coordinated by four  $8d$  and six  $8f$  neighbors. One of the  $8f$ - $8f$  distances, denoted  $d_1$  in Fig. 3, is significantly shorter than the others (compare Table I). Thus, the flat  $8f$  atom layers bear some resemblance to the two-dimensional dense packings of diatomic molecules encountered in halogen crystals with SG  $Cmca$ ,  $Z = 8$ .

The variation of selected interatomic distances with pressure is shown in Fig. 4(a). While  $d_1$  seems to remain constant with perhaps a small increase at higher pressure, the other distances decrease with increasing pressure. The long  $8f$ - $8d$  interlayer distance  $d_3$  has a value similar to that of atoms in neighboring hexagonal layers of hcp Si (2.5344 Å at 42.5 GPa). The values of other distances are close to those of the intralayer distances in both ph and hcp Si, with the exception of  $d_1$  which is similar to the closest atom separation in neighboring hexagonal layers of ph Si (2.3195 Å at 38.4 GPa). The interlayer bonds of the ph phase are known to have a large covalent admixture [12]. We have performed

TABLE I. Structural parameters for Si VI at different pressures. The orthorhombic unit cell contains 16 atoms. Free parameters are  $y, z$  (0,  $y, z$ ) and  $x$  ( $x, 0, 0$ ) for atoms in the Wyckoff  $8f$  and  $8d$  sites, respectively, of space group  $Cmca$ . The  $R(F^2)$  values refer to residuals for intensities and result from two-phase refinements of ph Si/Si VI or Si VI/hcp Si. Crystallographic data for Cs V [24] are listed for comparison.

$P$ (GPa)	38.4(Si)	42.5(Si)	45.5(Si)	12.0(Cs)
$a$ (Å)	8.0242(8)	7.9686(8)	7.9200(16)	11.205
$b$ (Å)	4.7961(5)	4.7759(5)	4.7586(8)	6.626
$c$ (Å)	4.7760(5)	4.7546(5)	4.7361(8)	6.595
$a/c$	1.680	1.676	1.672	1.699
$b/c$	1.004	1.004	1.005	1.005
$y(8f)$	0.173(5)	0.172(5)	0.173(10)	0.173
$z(8f)$	0.328(5)	0.328(5)	0.324(10)	0.327
$x(8d)$	0.218(5)	0.219(5)	0.224(10)	0.216
$R(F^2)$	0.05	0.075	0.086	...
Admixture	28% ph	4% hcp	55% hcp	...
$V_{\text{atom}}$ (Å <sup>3</sup> )	11.488(3)	11.308(3)	11.156(6)	30.603
$d_1$ (Å)	2.340(30)	2.321(30)	2.347(60)	3.237
$d_3$ (Å)	2.545(20)	2.525(20)	2.500(40)	3.612
$d_{\text{other}}$ (Å)	2.429–2.500	2.405–2.484	3.404–3.464	

tight-binding electronic structure calculations for Si VI [32]. Pronounced electron density maxima located at the midpoints of the short  $8f$ - $8f$  contacts indicate a covalent bonding contribution for the  $Si_2$  units.

The atomic volume of Si as a function of pressure is shown in Fig. 4(b). Values for Si VI at selected pressures are listed in Table I. At 38.4 GPa Si VI coexists with ph Si which at this pressure has  $V_{\text{atom}} = 12.108(3)$  Å<sup>3</sup>. For hcp Si at 42.5 GPa we have  $V_{\text{atom}} = 11.090(3)$  Å<sup>3</sup> [ $a = 2.4729(3)$  Å,  $c = 4.1880(4)$  Å,  $c/a = 1.693$ ]. Thus, there is sizable volume change by  $-5.4\%$  at the ph to Si VI transition. The hcp volume is only 1.9% smaller than that of Si VI at the same pressure. This suggests that the oC16 structure of Si VI falls into the category of densely packed structures.

Calculated total energies of Si in various structures with coordination numbers varying from 8 to 12 were found to be almost identical [15]. Based on the new structure reported here, *ab initio* structure optimizations were performed [33] and near 40 GPa the oC16 structure was found to be stable with respect to ph and hcp phases, in agreement with experiment.

The oC16 structure is incompatible with a ph to hcp transition mechanism based on a simple restacking of hexagonal layers driven by a soft phonon mode, as proposed in theoretical studies [12,13]. The ph structure can be described in SG  $Cmca$  with  $y = 1/4, z = 1/2$  for  $8f, x = 1/4$  for  $8d$ , and  $a/b = \sqrt{3}$ . Thus the continuous path from ph Si to Si VI involves a combination of atom displacements within ( $8f$ ) and perpendicular ( $8d$ ) to the layers. We point out a remarkable similarity in the structural sequence for Cs and Si. In both cases the oC16 phase occurs intermediate between 8-fold coordinated (Cs-IV, ph-Si) and hcp phases with  $c/a$  ratios close to 1.7. A difference is that the stability range of the oC16 structure in Cs extends over a much larger pressure range (12 to 72 GPa) compared to Si.

In conclusion, based on high-resolution monochromatic synchrotron x-ray diffraction data, we have solved the

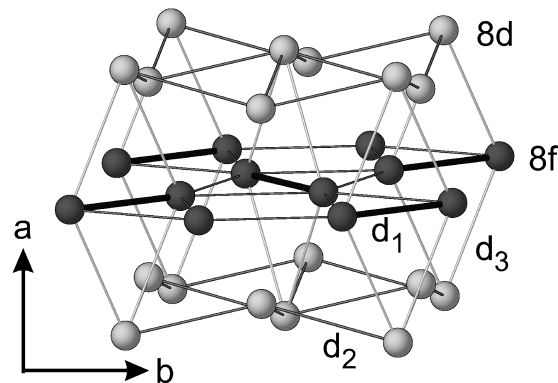


FIG. 3. A section of the oC16 crystal structure of Si VI showing the flat  $8f$  atom layers consisting of close-packed  $Si_2$  units and the strongly buckled nearly square  $8d$  atom layers. The  $d_i$ 's are characteristic bond lengths (see text).

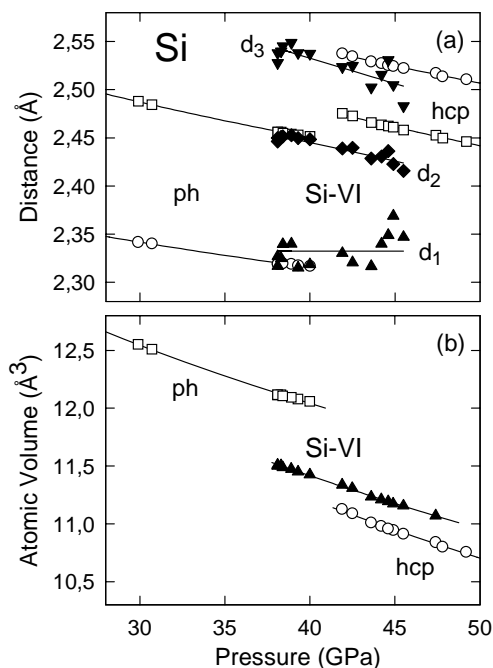


FIG. 4. (a) Characteristic interatomic distances  $d_1$ ,  $d_2$ , and  $d_3$  (compare Fig. 3) in Si VI versus pressure. Open circles and squares refer to the interlayer and intralayer atomic distances, respectively, of the ph and hcp phases. (b) The atomic volume of Si phases as a function of pressure. Lines in (a) and (b) are guides to the eye.

long-standing problem of the crystal structure of Si VI. The space group is determined as  $Cmca$  and the conventional unit cell contains 16 atoms. Si VI is found to be isostructural to Cs V. This not only applies to the overall crystal symmetry, but also to axial ratios and free atom position parameters. The oC16 structure, which does not occur in any elemental solid at ambient conditions, has now been observed at high pressure for two materials with quite different electronic configurations. It thus appears that the Cs V type structure plays a more general role of an intermediate structure during pressure-driven phase transitions from 8-fold coordination towards dense packing of atoms. We suggest to consider oC16 as a possible structure candidate in first-principles calculations of the phase stability of light elements at very high pressures.

We thank N.E. Christensen for communicating results of unpublished calculations.

[1] S. Minomura and H.G. Drickamer, *J. Phys. Chem. Solids* **23**, 451 (1962).  
 [2] J.C. Jamieson, *Science* **139**, 762 (1963).  
 [3] H. Olijnyk, S.K. Sikka, and W.B. Holzapfel, *Phys. Lett.* **103A**, 137 (1984).  
 [4] J.Z. Hu and I.L. Spain, *Solid State Commun.* **51**, 263 (1984).  
 [5] J.Z. Hu, L.D. Merkle, C.S. Menoni, and I.L. Spain, *Phys.*

*Rev. B* **34**, 4679 (1986).  
 [6] S.J. Duclos, Y.K. Vohra, and A.L. Ruoff, *Phys. Rev. Lett.* **58**, 775 (1987).  
 [7] S.J. Duclos, Y.K. Vohra, and A.L. Ruoff, *Phys. Rev. B* **41**, 12021 (1990).  
 [8] M.I. McMahon and R.J. Nelmes, *Phys. Rev. B* **47**, 8337 (1993); M.I. McMahon, R.J. Nelmes, N.G. Wright, and D.R. Allan, *Phys. Rev. B* **50**, 739 (1994).  
 [9] For a recent review see R.J. Nelmes and M.I. McMahon, in *High Pressure Semiconductor Physics I*, edited by T. Suski and W. Paul (Academic, New York, 1998), p. 145.  
 [10] M.T. Yin and M.L. Cohen, *Phys. Rev. Lett.* **45**, 1004 (1980).  
 [11] R.J. Needs and R.M. Martin, *Phys. Rev. B* **30**, 5390 (1984).  
 [12] K.J. Chang and M.L. Cohen, *Phys. Rev. B* **30**, 5376 (1984); **31**, 7819 (1985).  
 [13] K.J. Chang *et al.*, *Phys. Rev. Lett.* **54**, 2375 (1985).  
 [14] S.P. Lewis and M.L. Cohen, *Phys. Rev. B* **48**, 16144 (1993).  
 [15] R.J. Needs and A. Mujica, *Phys. Rev. B* **51**, 9652 (1995).  
 [16] R.O. Piltz *et al.*, *Phys. Rev. B* **52**, 4072 (1995).  
 [17] B.G. Pfommer, M. Côté, S.G. Louie, and M.L. Cohen, *Phys. Rev. B* **56**, 6662 (1997).  
 [18] M. Hanfland, M. Alouani, K. Syassen, and N.E. Christensen, *Phys. Rev. B* **38**, 12864 (1988).  
 [19] J.M. Mignot, G. Chouteau, and G. Martinez, *Phys. Rev. B* **34**, 3150 (1986).  
 [20] T.H. Lin *et al.*, *Phys. Rev. B* **33**, 7820 (1986).  
 [21] D. Erskine, P.Y. Yu, K.J. Chang, and M.L. Cohen, *Phys. Rev. Lett.* **57**, 2741 (1986).  
 [22] Y.K. Vohra *et al.*, *Phys. Rev. Lett.* **56**, 1944 (1986).  
 [23] V. Vijaykumar and S.K. Sikka, *High Press. Res.* **4**, 306 (1990).  
 [24] U. Schwarz, K. Takemura, M. Hanfland, and K. Syassen, *Phys. Rev. Lett.* **81**, 2711 (1998).  
 [25] H.K. Mao, J. Xu, and P.M. Bell, *J. Geophys. Res.* **91**, 4673 (1986).  
 [26] C. Schulze *et al.*, *J. Synchrotron Radiat.* **5**, 77 (1998).  
 [27] A.P. Hammersley *et al.*, *High Press. Res.* **14**, 235 (1996).  
 [28] M. Ross, H.K. Mao, P.M. Bell, and J.A. Xu, *J. Chem. Phys.* **85**, 1028 (1986).  
 [29] All observed  $d$  values reported in Ref. [7] for a pressure given as 40 GPa are consistent with the  $Cmca$  ( $Z = 16$ ) structure, resulting in a volume of  $11.24 \text{ \AA}^3/\text{atom}$ . Based on the present results this volume corresponds to a pressure of 44 GPa.  
 [30] A.C. Larson and R.B. von Dreele, GSAS—General structure analysis system, Los Alamos National Laboratory Report No. LAUR 86-748.  
 [31] The March-Dollase ellipsoid [30] was oriented along the incident beam, and the preferred orientation axis was [100]. The ellipsoid axes ratio was 0.73 at 42.5 GPa. Without allowance for preferred orientation we obtain  $R(F^2) = 19\%$ ,  $y(8f) = 0.1728$ ,  $z(8f) = 0.3267$ , and  $x(8d) = 0.2181$ . These  $x, y, z$  parameters agree within accuracy of the measurement with those listed in Table I.  
 [32] U. Schwarz, O. Jepsen, and K. Syassen (unpublished).  
 [33] N.E. Christensen and D.L. Novikov (private communication).